Metabolic Responses of "Big Six" *Escherichia coli* in Wheat Flour to Thermal Treatment Revealed by Nuclear Magnetic Resonance Spectroscopy

Yue Wang,[a,b] Disheng Zhou,[a,b] ⓘHongshun Yang[a,b]

[a]Department of Food Science and Technology, National University of Singapore, Singapore, Singapore
[b]National University of Singapore (Suzhou) Research Institute, Suzhou, Jiangsu, People's Republic of China

ABSTRACT *Escherichia coli* outbreaks linked to wheat flour consumption have kept emerging in recent years, which necessitated an antimicrobial step being incorporated into the flour production process. The objectives of this *in vivo* study were to holistically evaluate the sanitizing efficacy of thermal treatment at 60 and 70°C against the "big six" *E. coli* strains (O26:H11, O45:H2, O103:H11, O111, O121:H19, and O145) in wheat flour and to assess the strain-specific metabolic responses using nuclear magnetic resonance (NMR) spectroscopy. The 70°C treatment temperature indiscriminatingly inactivated all strains by over 4.3-log CFU/g within 20 min, suggesting the high sanitization effectiveness of this treatment temperature, whereas the treatment at 60°C inactivated the strains to various degrees during the 1-h process. The most resistant strains at 60°C, O26 and O45, were characterized by amino acid and sugar depletion, and their high resistance was attributed to the dual effects of activated heat shock protein (HSP) synthesis and promoted glycolysis. O121 also demonstrated these metabolic changes, yet its thermal resistance was largely impaired by the weakened membrane structure and diminished osmotic protection due to phosphorylcholine exhaustion. In contrast, O111, O145, and O103 presented a substantial elevation of metabolites after stress at 60°C; their moderate thermal resistance was mainly explained by the accumulation of amino acids as osmolytes. Overall, the study enhanced our understanding of the metabolic responses of big six *E. coli* to heat stress and provided a model for conducting NMR-based metabolomic studies in powdered food matrices.

IMPORTANCE "Big six" *Escherichia coli* strains have caused several outbreaks linked to wheat flour consumption in the last decade, revealing the vital importance of adopting an antimicrobial treatment during the flour production process. Therefore, the present study was carried out to evaluate the efficacy of a typical sanitizing approach, thermal treatment, against the big six strains in wheat flour along with the underlying antimicrobial mechanisms. Findings showed that thermal treatment at 60 and 70°C could markedly mitigate the loads of all strains in wheat flour. Moreover, activated heat shock protein synthesis combined with expedited glycolysis and enhanced osmotic protection were identified as two major metabolic alteration patterns in the *E. coli* strains to cope with the heat stress. With the responses of big six in wheat flour to thermal treatment elucidated, scientific basis for incorporating a thermal inactivation step in wheat flour production was provided.

KEYWORDS *Escherichia coli*, flour, NMR, foodomics

Wheat, an energy-dense crop containing up to 71% carbohydrates and 10% gluten protein, is a staple food of the world's population (1, 2). Being cultivated on more lands than any other crops, north to Scandinavia and Russia and south to Argentina,

including elevated regions in the tropical areas (3), wheat was produced at 766 million tons in 2019, only second to maize (1,148 million tons) (4, 5). While the high-calorie property and the wide production set the foundation for wheat to dominate people's diets, the superior ability to be processed further consolidates its position on people's dining table. Flour is a commercial form of wheat; it can be processed into a huge variety of food commodities, such as bread and pasta in Western diets and noodles in Eastern diets, which largely enriches people's food choices.

Foods made from wheat flour are normally consumed cooked, with boiling, baking, steaming, and frying being the most common household cooking means. While the high-temperature cooking processes are designed to enhance flavors, they simultaneously function as an antimicrobial step that wipes out microbiological hazards present in wheat. Owing to this, a standard antimicrobial process is typically omitted in traditional wheat flour production (6). However, the drawbacks of such omission have been revealed in recent outbreaks, an example being the one in 2016, which led to 63 infections, 17 hospitalizations, and one hemolytic uremic syndrome (HUS) case (7). The outbreak was caused by Shiga toxin-producing *Escherichia coli* (STEC) O121 and O26. Among 38 ill people interviewed, 19 (50%) reported eating or tasting raw, homemade dough or batter. Although governments have warned the public not to eat uncooked flour, it was palliative, as a later outbreak in 2019 caused by *E. coli* O26 and another one earlier this year caused by *E. coli* O121 again highlighted eating raw dough or batter among the ill (8, 9). These incidences clearly stressed the need to incorporate solid antimicrobial interventions in wheat flour production to ensure that pathogens are eliminated before flour is put on the market.

Based on the reported outbreaks, STEC are key culprits for wheat flour contamination, and among them, the serotypes commonly known as the "big six" (O26, O103, O111, O121, O45 and O145) are of special concern (10). To mitigate the load of big six in wheat flour, thermal treatment is no doubt the most applicable approach, since it does not bring in water to affect the moisture content and texture of the low-water-activity (a_w) food. The efficacy of this conventional sanitizing technique against common foodborne pathogens has been extensively documented. For instance, a 5-min thermal treatment at 60°C was found to effectively reduce *E. coli* O157 in broth by 3.78 log CFU/mL, and the same setting also showed effectiveness against *Listeria monocytogenes* strains on salmon (11, 12). The effects of thermal treatment on disinfecting big six in flour have also been explored in some studies (13–16); however, with limited knowledge about the mechanisms underlying the antibacterial process, application of heat treatment to decontaminate flour in real life was not examined.

Metabolomics has been increasingly involved in the food science field for mechanism study. Among the emerging tools, nuclear magnetic resonance (NMR) spectroscopy, able to acquire snapshots of the comprehensive bacterial metabolic profiles under external stresses, is applied with high popularity (17). It has been applied to investigate the metabolic variations occurring in *L. monocytogenes* on shrimp after the combined antimicrobial treatment of nisin and grape seed extract (18). It has also been used to detect the metabolic responses of *E. coli* O157, *L. monocytogenes*, and *L. innocua* on fresh vegetables under electrolyzed water sanitizing treatment (19, 20). On this basis, NMR spectroscopy may provide insights in understanding the heat-induced metabolic responses of big six in wheat flour as well.

To perform NMR analysis, microbial cells must be first separated from the food sample before the cell metabolites are extracted for analysis. However, compared to fruit and vegetables from which microbial cells can be rinsed out directly, the powdered format of flour makes the microbe isolation a difficult task; consequently, flour has always been circumvented in metabolomic studies in the past. This study is the first time that microorganisms in wheat flour are recovered and subject to metabolomic analysis, and the recovery procedure would serve as a template for future microbial metabolomic studies carried out on powdered foods. With interests in the responses of big six in wheat flour to heat stress, the present study was undertaken to assess the
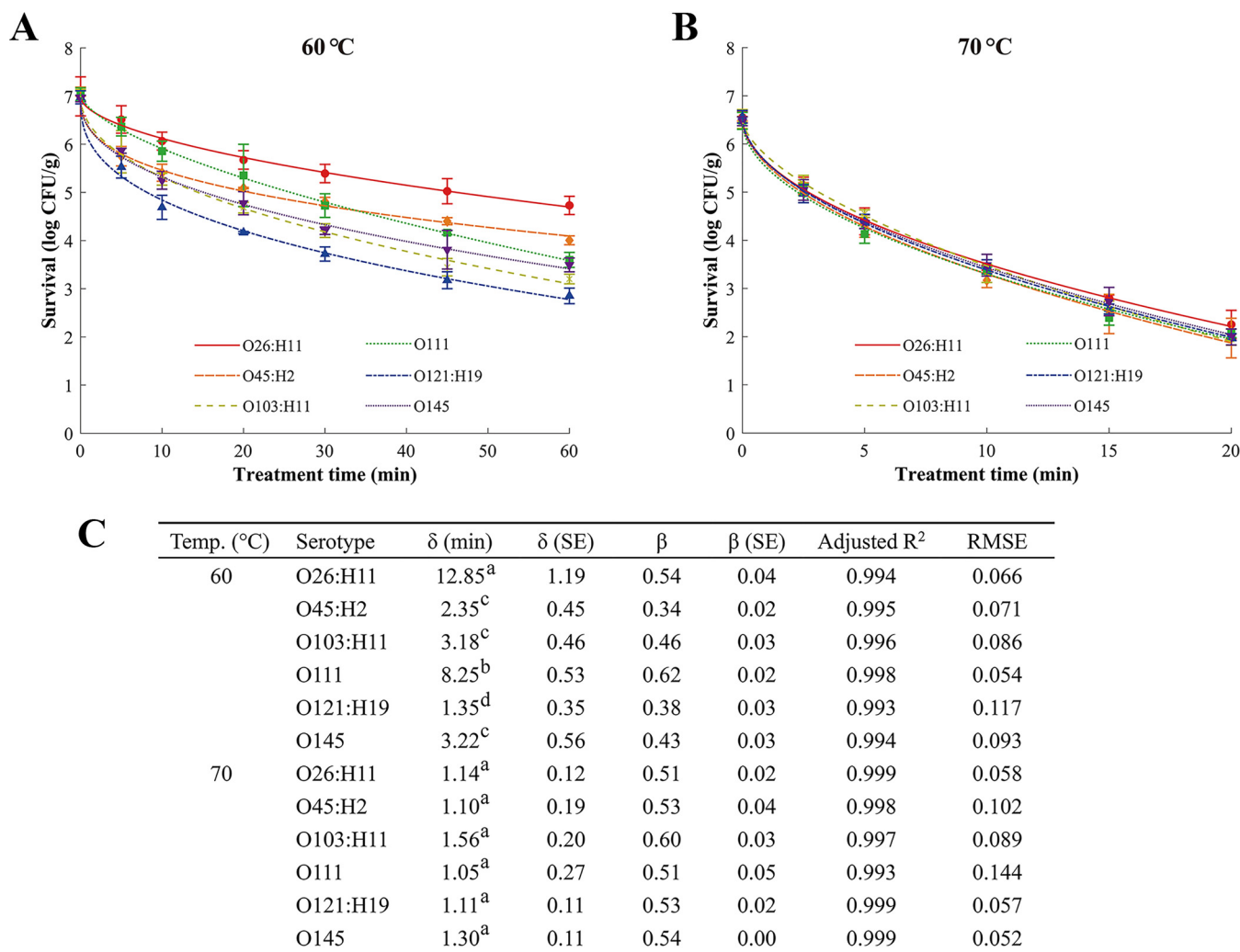
FIG 1 Thermal inactivation curves of *E. coli* O26:H11, O45:H2, O103:H11, O111, O121:H19, and O145 in wheat flour at 60°C for up to 60 min (A) and 70°C for up to 20 min (B), and the corresponding inactivation kinetics parameters were calculated by Weibull model (C). Survivals are presented as means ± standard deviation (*n* = 6). δ values for the same treatment temperature followed by different letters are significantly different (*P* < 0.05).

viability of each individual big six *E. coli* serotype in wheat flour under thermal treatment. By revealing the metabolic changes in the strains underlying the antimicrobial process, additional scientific basis for incorporating a thermal treatment step in flour production would be provided.

RESULTS AND DISCUSSION

Sanitizing efficacy of thermal treatment against *E. coli* strains in wheat flour. As shown in Fig. 1A, when the inoculated wheat flour samples were heat treated at 60°C, the viable counts of the six *E. coli* strains (O26:H11 [ATCC BAA-2196], O45:H2 [ATCC BAA-2193], O103:H11 [ATCC BAA-2215], O111 [ATCC BAA-2440], O121:H19 [ATCC BAA-2219], and O145 [ATCC BAA-2192]) decreased markedly from 7.01 ± 0.20 log CFU/g at 0 min to an average of 3.65 log CFU/g by the end of the process. The O26 and O45 strains were the only two inactivated by less than 3 log CFU/g, which had final surviving populations of 4.73 ± 0.19 and 4.01 ± 0.09 log CFU/g, respectively. The treatment was more effective against the O111 and O145 strains, resulting in significantly reduced survival to 3.60 ± 0.16 and 3.49 ± 0.14 log CFU/g, respectively (*P* < 0.05). Higher lethality was observed in the O103 strain, with 3.20 ± 0.10 log CFU/g surviving the treatment. Moreover, with a final surviving count of only 2.85 ± 0.16 log CFU/g, the O121 strain was the least resistant among the six at 60°C.

Generally, the inactivation rate of *E. coli* increases drastically as the treatment temperature increases. For instance, Suehr et al. reported that the logarithmic reduction (*d* value) of *E. coli* O121 in wheat flour was achieved at 18.16, 6.47, and 4.58 min when treated at 70, 75, and 80°C, respectively (21). Consistent with this, upon elevating the treatment temperature to 70°C in our study, a more than 4.30-log CFU/g reduction of all six strains was achieved within 20 min (Fig. 1B). In fact, the six strains had similar survival counts at multiple sampling time points during the treatment process; therefore, significant overlap was observed in their thermal inactivation curves. These observations indicated that the heat stress imparted at 70°C had comparable effectiveness against the big six members. A recent study by Daryaei et al., which reported massive inactivation of all tested *E. coli* strains in wheat flour stressed at 82°C for 5 min, further revealed that the inactivation capability of a sufficiently high temperature was irrelevant to the *E. coli* serotype (14). Since the treatment only lasted 20 min and the inactivation curves did not reach a plateau by the end, complete inhibition of the *E. coli* cells seemed to be achievable if the treatment process was slightly extended. Although stressful enough for wiping out the big six in wheat flour, the relatively mild temperature and short treatment time in combination was unlikely to affect the functional properties of wheat flour (22, 23), which was an additional advantage of the 70°C thermal treatment. In industrialized flour production, wheat flour may be heated to the desired temperature in rotating drums or heated conveyors, with the right time of heating calculated via unsteady-state heat transfer to the cold spot.

The Weibull model provides more information of the antimicrobial effect of thermal treatment on different strains in wheat flour (Fig. 1C). Previous studies have demonstrated that the Weibull model was a good fit for describing the kinetics of *E. coli* inactivation in food samples (24, 25). The high adjusted R^2 values (>0.99) and low root mean standard errors (RMSE) (<0.15) obtained in this study further confirmed the suitability of the Weibull model for describing *E. coli* inactivation. At 70°C, the δ of different strains were comparable, with the longest (O103) and the shortest (O111) differing by only 0.51 min and all of them staying under 1.56 min. The generic effectiveness of the 70°C thermal treatment in eliminating these potent STEC was once again evidenced. On the contrary, the 60°C treatment led to hugely differing δ values among the strains, from the longest in O26 (12.85 min) to the shortest in O121 (1.35 min). This also illustrated the highest and lowest tolerance of O26 and O121, respectively, to the temperature. The outstanding thermal resistance of O26 in wheat flour has also been documented in previous studies, where this serotype showed longer δ than the other big six members and even O157 at 60°C (15, 16). Contradicting our expectations, the second most resistant strain at 60°C, O45, had a relatively short δ. Several studies have shown that thermotolerance was gradually acquired in bacteria with extended heating time (26, 27). Thus, it was possible that a large number of O45 cells were killed before the strong defense mechanisms were fully launched. The gradual establishment of thermal defense mechanisms was also reflected in the concave shape of the surviving curves ($\beta < 1$) (Fig. 1A and B). In fact, bacterial cells surviving a sublethal stress would initiate a series of corresponding metabolic alterations as an instinct to enhance their chance of survival in subsequent stresses (28). Therefore, it was no wonder that the slowing downtrend in cell reduction was observed.

Experimental settings for metabolomic analysis. Metabolomic analysis can provide useful information regarding the dynamic metabolic changes in the *E. coli* strains during the treatment process. In spite of the great challenge of recovering *E. coli* cells from wheat flour, an *in vivo* setting was chosen for the metabolomic experiments based on its necessity in the following two main aspects. First, the composition of foods was proven to have an impact on the metabolic responses of microbes. For example, previous studies have shown that the fatty acid component of shrimp, in addition to providing better nutritional support for the survival of *L. monocytogenes* than TSB, also resulted in fewer metabolic perturbations in the living *Listeria* cells during the same sanitizing treatment (17, 29). On this basis, findings from an *in vitro* study

Metabolomic experimental setting	Option	Experimental basis	Comments
Temperature	60 °C	Reduced *E. coli* load by an average of 3.36 log CFU/g within 60 min.	Sufficient amount of *E. coli* cells with stress-induced metabolic changes could survive.
	70 °C	Reduced *E. coli* load by an average of 4.48 log CFU/g within 20 min.	*E. coli* cells might not have sufficient time to establish metabolic responses before they were inactivated.
Wheat flour size	10 g		High *E. coli* recovery. Metabolites could be gathered to sufficient levels so as to generate strong enough signals on NMR spectra.
	20 g		Moderate *E. coli* recovery. Exist risks of not detecting the signals of certain metabolites on NMR spectra.
	50 g		Low *E. coli* recovery. Too low metabolite levels to pass the detection threshold of NMR. The precipitate after high-speed centrifugation still contained a large portion of wheat flour.
	100 g		Low *E. coli* recovery. Metabolite levels might not pass the detection threshold of NMR. The precipitate after high-speed centrifugation still contained a large portion of wheat flour.

FIG 2 Experimental setting optimization for metabolomic analysis. Columns with different letters on top are significantly different ($P < 0.05$).

may be of limited reference value in predicting the microbial metabolic responses in real food decontamination processes. For wheat flour specifically, on the one hand, it is a typical carbohydrate- and gluten-rich food, so it could serve as an inexhaustible source of carbon and nitrogen for the residing *E. coli* cells (30). On the other hand, its low a_w would threaten the proliferation of *E. coli*, which has no growing capability at a_w of <0.95 (56). The two factors of wheat flour can exert obvious but contradicting effects on *E. coli*, making the heat-induced metabolic responses in *E. coli* cells unpredictable.

Second, wheat flour may have a hindrance effect on the microbes being sanitized (31). Unlike the germs found on the surface of fresh fruits and vegetables that are exposed to the external stresses directly (32–35), bacterial cells in wheat flour are typically well dispersed and completely hindered by wheat flour granules, which are several orders of magnitude larger. This required an external stress to penetrate the thick layer before reaching the *E. coli* cells to inactivate them; the power of stress could be impaired during the process, potentially resulting in milder metabolic responses in *E. coli* compared to that observed in studies conducted with fresh produce. Therefore, only metabolomic experiments carried out in the *in vivo* setting would accurately mimic *E. coli*'s metabolic responses during flour sanitization.

To obtain effective metabolomic results underlying the antimicrobial process, some minor factors to proceed with the metabolomic part also needed to be carefully optimized. As shown in Fig. 2, first was the thermal treatment temperature, for it determined whether the metabolic variations could be detected. Reflecting on the sanitizing effects in "Wheat flour inoculation," below, treatment at 70°C massively and indiscriminately killed the STEC cells within a short period of time. This was not a merit of metabolomic analysis, however, as the strains may not have developed decent defense

mechanisms before they were killed. The treatment at 60°C, in comparison, imposed milder stress to the cells; it killed the STEC cells at a much slower pace, which enabled the sublethal cells to gain tolerance to the stress and build up corresponding defense mechanisms during the treatment period (19, 36). As a consequence, stress-induced metabolic changes could be viewed in a sufficient number of surviving cells. Additionally, as the metabolomes might change dynamically during the treatment process, the metabolomes of each strain stressed for 5 and 60 min were captured at that temperature and were compared with the ones at 0 min to unravel the initial and lasting metabolic responses of each strain to the heat stress.

The other important factor to consider was the sample size of the wheat flour being inoculated, for it primarily decided the difficulty level of recovering *E. coli* cells from the homogenized *E. coli*–wheat flour mixture. In the optimization experiment, the *E. coli* recovery rates from different amounts (10, 20, 50, and 100 g) of wheat flour were examined. As shown on the histogram (Fig. 2), the percent recovery was negatively correlated with the sample size, where the *E. coli* cell recovery from 10 g of wheat flour (81.8% $\pm$ 1.3%) far outweighed that from the larger sample sizes. A possible rationale was that when *E. coli* cells were surrounded by larger amounts of wheat flour, during low-speed centrifugation, the difficulty for the cells to escape from the bulky mixture to the upper liquid portion would be higher; thus, more cells would precipitate together with the flour, leading to a lower percent recovery. Worse still, the low recovery would lead to low metabolite signals on the NMR spectra, which would undoubtedly impair the accuracy of metabolite quantification and even cause fewer metabolites to be identified if their concentrations did not pass the detection threshold of NMR. Based on these findings, 10 g was selected as the size of the wheat flour sample to be inoculated for subsequent metabolomic analysis.

Metabolic profiles of *E. coli* strains in wheat flour. Representative ^{1}H NMR spectra of the six strains stressed at 60°C for 0, 5, and 60 min are shown in Fig. S1 in the supplemental material. Cooperatively referring to the two-dimensional (2D) ^{1}H–^{13}C spectra, metabolic databases, and the literature, a total of 30 metabolites were identified in all strains (Table S1), which was in accordance with the set of metabolites in the big six isolated from TSB in a previous study (17). Amino acids (e.g., leucine, isoleucine, valine, alanine, arginine, and methionine) and organic acids (e.g., lactic acid, acetic acid, and α-ketoglutaric acid) dominated the high field region (0.5 to 4.0 ppm) of the spectra. Ethanol and betaine were assigned in this region as well. In the lower field region (4.0 to 10.0 ppm), most signals belonged to sugars (e.g., α-D-glucose, β-D-glucose, and glucose-1-phosphate) and nucleotide-related compounds (e.g., ATP, ADP, and adenosine).

Despite the high similarity in metabolic composition, diversity in metabolites' signal intensity existed among the strains and treatment time. For visualization of the relative metabolite abundance, the signals of 23 metabolites with no overlapping chemical shifts were quantified, and a heatmap was plotted on a blue-red color scale (Fig. 3). Lactic acid, shown in a spectrum of red colors, represented the most dominant metabolite in all samples. In contrast, nucleotide-related compounds, including ATP, adenosine, and uridine, mainly presented in bluish colors, represented the minor components of the *E. coli* metabolome. Furthermore, 11 amino acids were quantified in the *E. coli* samples, among which alanine was the rarest. According to the color transition, the low concentration of alanine was slightly compensated throughout thermal treatment in O26, O45, and O145, whereas it was further depleted in O103, O111, and O121.

Temporal changes of metabolic profiles of *E. coli* strains in wheat flour. An overview of the endogenous metabolic alterations of all strains throughout the 60°C thermal treatment was generated by PCA, which compared the metabolic profiles of the six strains recovered from the flour treated for 0 min, 5 min, and 60 min. Clear separation of the profiles was illustrated, where the first three principal components (PCs) explained 84.6% of the total data (PC1, 42.7%; PC2, 25.1%; PC3, 16.8%) with good model fitness ($Q^2 = 0.78$) (Fig. 4A).

Based on the first two PCs, the metabolic trajectory of each strain was plotted by connecting the mean coordinates in the score plot chronologically (Fig. 4B). In this
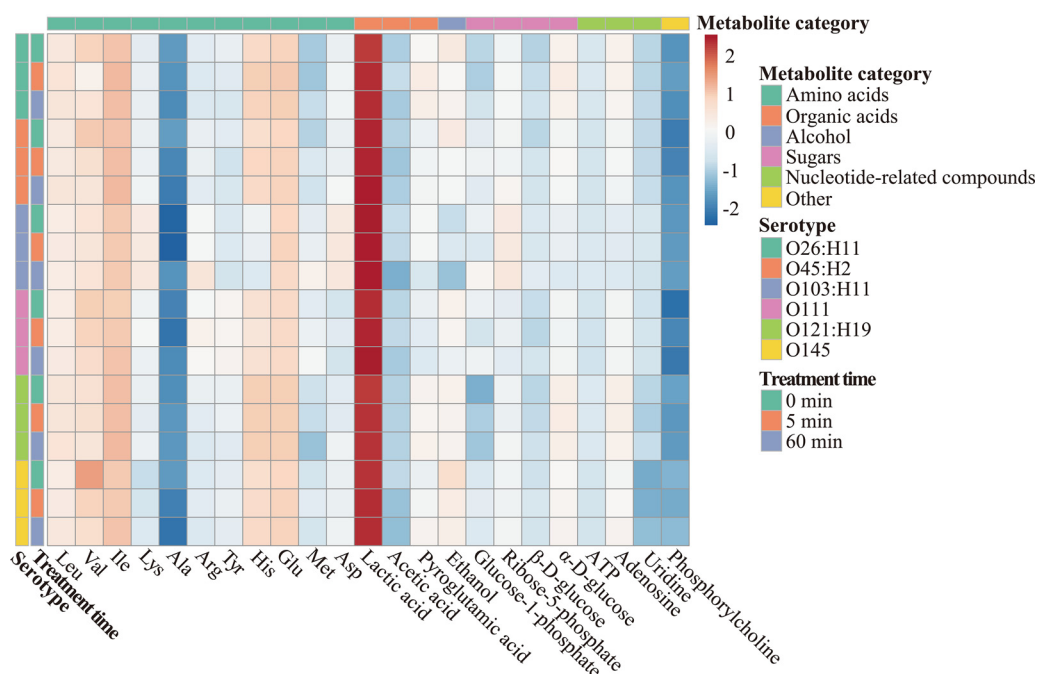
FIG 3 Heatmap of metabolites in *E. coli* O26:H11, O45:H2, O103:H11, O111, O121:H19, and O145 in wheat flour treated at 60°C for 0, 5, and 60 min.

plot, each metabolic profile was denoted as a single point from which the magnitude and pattern of each strain's metabolic changes during treatment could be visualized. Among all strains, the one from O103 presented the largest magnitude of metabolic variation during the heating process, as its metabolic profile deviated the longest distance along PC1 and moved from the negative side to the positive side of PC2. Axis crossing was also observed in O111's and O145's trajectories, which crossed PC1 and PC2, respectively. Combining with the observations in Fig. 1A that the reductions of the three strains were within the range of 3 to 4 log CFU/g, which represented moderate thermal resistance among the six, the large magnitude of metabolic changes indicates the launching of decent thermal defense mechanisms in the strains. In contrast, the metabolic trajectories of the O26 and O45 strains were confined to the second quadrant; as they moved downwards throughout the 60-min heating process, they both became less affected by PC2. Interestingly, the two strains were also those demonstrating the highest thermal resistance in "Sanitizing efficacy of thermal treatment
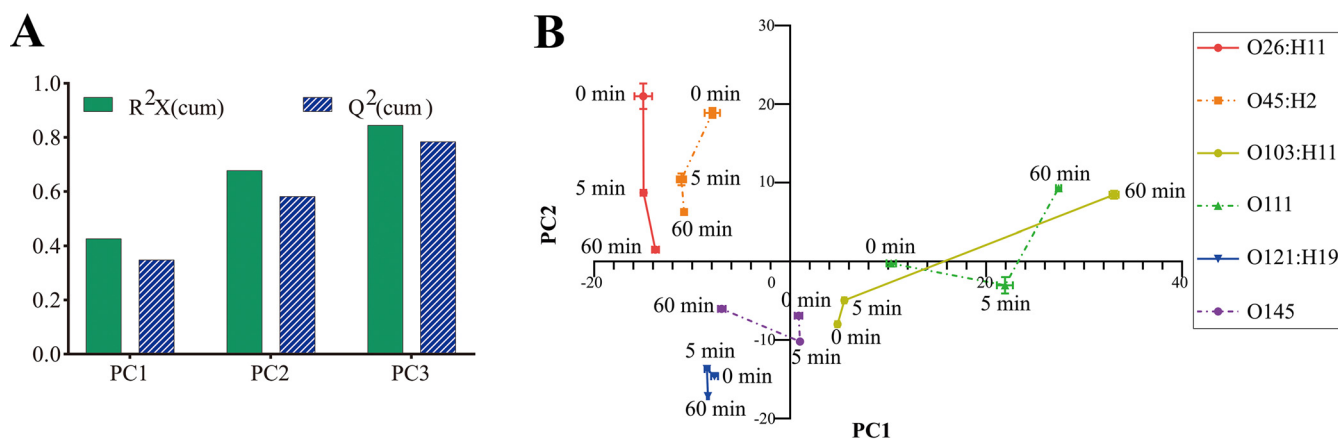

FIG 4 Principal-component analysis (PCA) of ^{1}H NMR spectra of *E. coli* O26:H11, O45:H2, O103:H11, O111, O121:H19, and O145 in wheat flour treated at 60°C for 0, 5, and 60 min. Principal components were explained for the variances (A) and trajectory plot (B).

against *E. coli* strains in wheat flour," above, which implied that this similar metabolic alteration pattern offered them a similarly high level of protection against the heat stress. Lastly, as the O121 strain presented minimal metabolic profile shifting, a failure in adequate defense mechanism implementation was suspected in the strain, which was incongruent with vast elimination of viable cells observed in "Sanitizing efficacy of thermal treatment against *E. coli* strains in wheat flour," above.

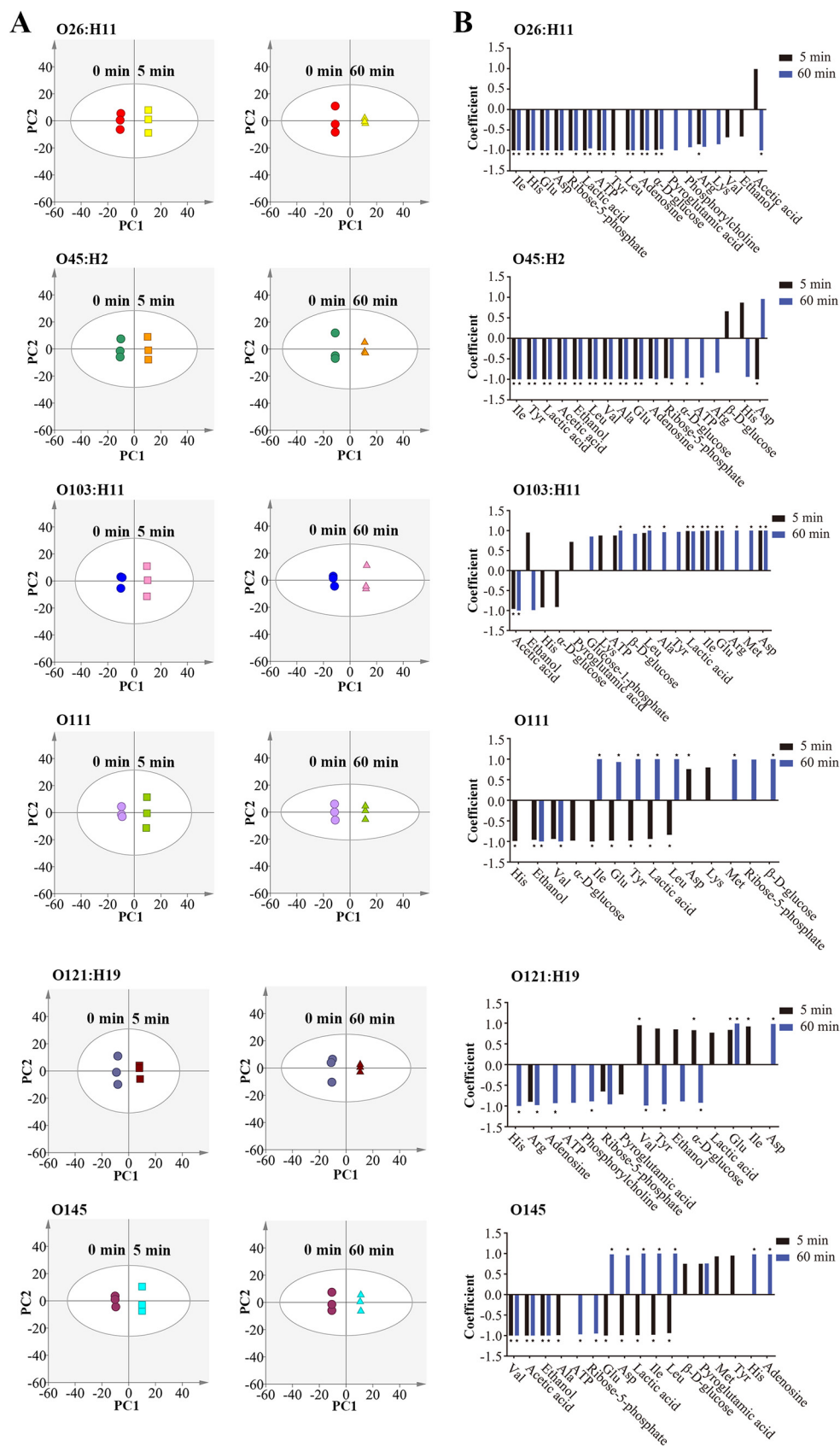**Alternative metabolites in *E. coli* strains in wheat flour under thermal treatment.** While the PCA results primarily manifested the inextricable linkage between the strains' thermal resistance and their heat-induced metabolic alterations, a more supervised model, orthogonal projection to latent structures-discriminant analysis (OPLS-DA), was applied to pairwise samples to examine the specific differences in their metabolomes. For each strain in wheat flour treated at 60°C, the metabolomes at 5 min and 60 min were separately compared with that obtained at 0 min, the control. All established OPLS-DA models demonstrated good predictability and interpretability, as guaranteed by the R^2Y and Q^2 values, respectively (Table S2) (17). Their robustness was further verified with the 200-iteration permutation test in which the order of the categorical variable Y was randomly permuted. As shown in Fig. S2, with all permuted Q^2 to the left lower than the original values to the right and the Q^2 regression lines intersecting the vertical axis below zero, the criteria for validity of the original models were met, which proved that the original OPLS-DA models were not overfitted and random (37).

The score plots showed significant intergroup metabolomic differences (Fig. 5A), indicating that heating for as short as 5 min could lead to detectable changes in *E. coli*'s metabolome. The prominent metabolites that differentiated the paired samples were screened based on their correlation coefficient and variable importance in projection (VIP) values obtained from the OPLS-DA models. All metabolites with correlation coefficient of >0.602 were filtered and presented in Fig. 5B, and those that simultaneously fulfilled the criteria of VIP value of >1 and P value of <0.05 were deemed the significant discriminative metabolites and depicted with stars.

A universal depletion of metabolites was observed in O26 and O45, with most declination occurring within 5 min (Fig. 5B). A major difference between the two was that the levels of α-D-glucose and nucleotide-related compounds (e.g., ATP and adenosine) were decreased in O26 from 5 min onwards, while they were decreased in O45 only at 60 min. The swift decrease of metabolites in O26 represented a prompt defense reaction toward the stress, which may explain the significantly longer δ in O26 than O45 (Fig. 1C). In contrast, O103 illustrated an opposite pattern of metabolic variation. Except for the decrease in acetic acid observed from 5 min, all other metabolites varied, which included an array of amino acids (e.g., leucine, isoleucine, glutamic acid, and aspartic acid), lactic acid, and ATP, presented an upward tendency.

While the aforementioned strains had their metabolite levels altered in a single direction during the whole course of thermal treatment, the temporal changes in the other three strains' metabolomes were more complicated. In O111 and O145, multiple amino acids (e.g., leucine, isoleucine, and glutamic acid) and lactic acid underwent a significant decrease transiently at 5 min (Fig. 5B). This momentary depression of metabolite levels might be the instantaneous reactions of the strains to the sudden elevation of temperature, causing the rapid cell reductions within a short time. After that, the metabolite levels rebound, which was associated with steadier cell reductions, suggesting that adequate metabolic adjustments were gradually made for the two strains to antagonize the heat stress. As for O121, in accord with the short displacement on the trajectory plot (Fig. 4B), only four metabolites (isoleucine, valine, glutamic acid, and α-D-glucose) were markedly affected at 5 min, and depletion of metabolites (e.g., tyrosine, histidine, α-D-glucose, and phosphorylcholine) was observed only in its 60-min metabolome (Fig. 5B).

Alterative metabolic pathways in *E. coli* strains in wheat flour under thermal treatment. Based on the screened metabolites that significantly discriminated each strain at the beginning of the treatment (0 min) and at the end of the treatment

FIG 5 Orthogonal projection to latent structures-discriminant analysis (OPLS-DA) score plots (A) and coefficient plots (B).

(60 min), perturbations in the strains' metabolic networks during the thermal treatment course were examined by MetaboAnalyst 5.0. The significantly affected pathways ($P < 0.05$) in each strain are listed in Table S3 and marked as circles in Fig. 6. Several pathways were disturbed universally. For instance, aminoacyl-tRNA biosynthesis, the pathway in amino acid metabolism responsible for correct pairing of an amino acid with its cognate tRNA, and carbapenem biosynthesis, the pathway for antibiotic synthesis in which glutamic acid is an intermediate, were significantly altered in all six strains. Additionally, biosynthesis and degradation of valine, leucine, and isoleucine as well as alanine, aspartic acid, and glutamic acid metabolism were each significantly changed in five strains (O26, O45, O103, O111, and O145; O26, O45, O103, O121, and O145). Glycolysis/gluconeogenesis, arginine biosynthesis, and pyruvate metabolism were each significantly changed in four strains (O26, O45, O111, and O145; O26, O103, O121, and O145; O26, O45, O103, and O145).

Referring to the Kyoto Encyclopedia of Genes and Genomes (KEGG) database, a schematic showing the metabolic changes of the six strains, along with the possible rationale for each strain's thermal resistance, are summarized in Fig. 7. In general, the metabolic perturbations between O26 and O45 showed high similarities, while those among O103, O111, and O145 were also relatively consistent.

Associated with the dynamic change of amino acid contents, amino acid metabolism was the most disturbed pathway in all *E. coli* strains studied. The finding was in accordance with previous studies, which documented the particularly high sensitivity of amino acid metabolism in various microorganisms to external stresses, including heat, oxidation, and acidity (11, 12). On one hand, the O26, O45, and O121 strains presented a substantial reduction in an array of amino acids. This was unsurprising indeed, since the amino acids might be used largely for synthesizing heat shock proteins (HSPs). HSPs, mostly molecular chaperones, can be synthesized in all species when cells are briefly exposed to temperatures above normal growth temperature (38). In *E. coli* specifically, the primary chaperone machinery contains DnaK, DnaJ, and GrpE (39). They facilitate acclimating the cells to the elevated temperatures by degrading denatured and misfolded proteins, inhibiting irreversible aggregation of unfolded proteins, and restoring proteins to their native structures at the cost of depleting amino acids (40). Apart from HSP production, energy deficiency might be another causative factor for the amino acid reduction. Based on previous studies, energy expenditure was expedited in response to heat stress (41, 42). Concomitantly, as an ATP-dependent process was energy supply retarded, amino acid synthesis would lack sufficient support (43). Furthermore, amino acid reduction also indicates decreased cell activity (44). For instance, glutamic acid, an amino acid that serves as a primary precursor in multiple biosynthesis pathways, was found to be synthesized abundantly in actively growing cells (45). The downregulation of glutamic acid in O26 and O45, therefore, revealed a lowered cell activity of the strains under the heat stress.

On the other hand, the O103, O111, and O145 strains were highlighted with significantly upregulated amino acid contents. Possible sources of the amino acids include breakdown of abnormal, misfolded proteins under heat stress and degradation of some proteins for the synthesis of new proteins vital at high temperatures (46). As many amino acids (e.g., leucine, alanine, and glutamic acid) are natural osmotic regulators that help sustain cytoplasmic osmolarity and prevent collapse of subcellular structures (47), their accumulation indicated enhanced osmotic protection in these strains. As was mentioned before, O103, O111, and O145 presented moderate thermal resistance among the six serotypes, which suggested that relieving osmotic pressure was a mediocre strategy for survival compared with those focusing on producing HSPs.

Amino acids are important carbon and energy sources in *E. coli* (17). The depletion of amino acids in O26, O45, and O121 therefore necessitated the strains to turn to alternative sources for energy supply. Glucose is the core energy source of *E. coli* under detrimental circumstances. Previous study has shown that the transcription of glycolysis genes, including *pgi*, *pgk glk*, and *pykF*, that encode glucose-6-phosphate isomerase,
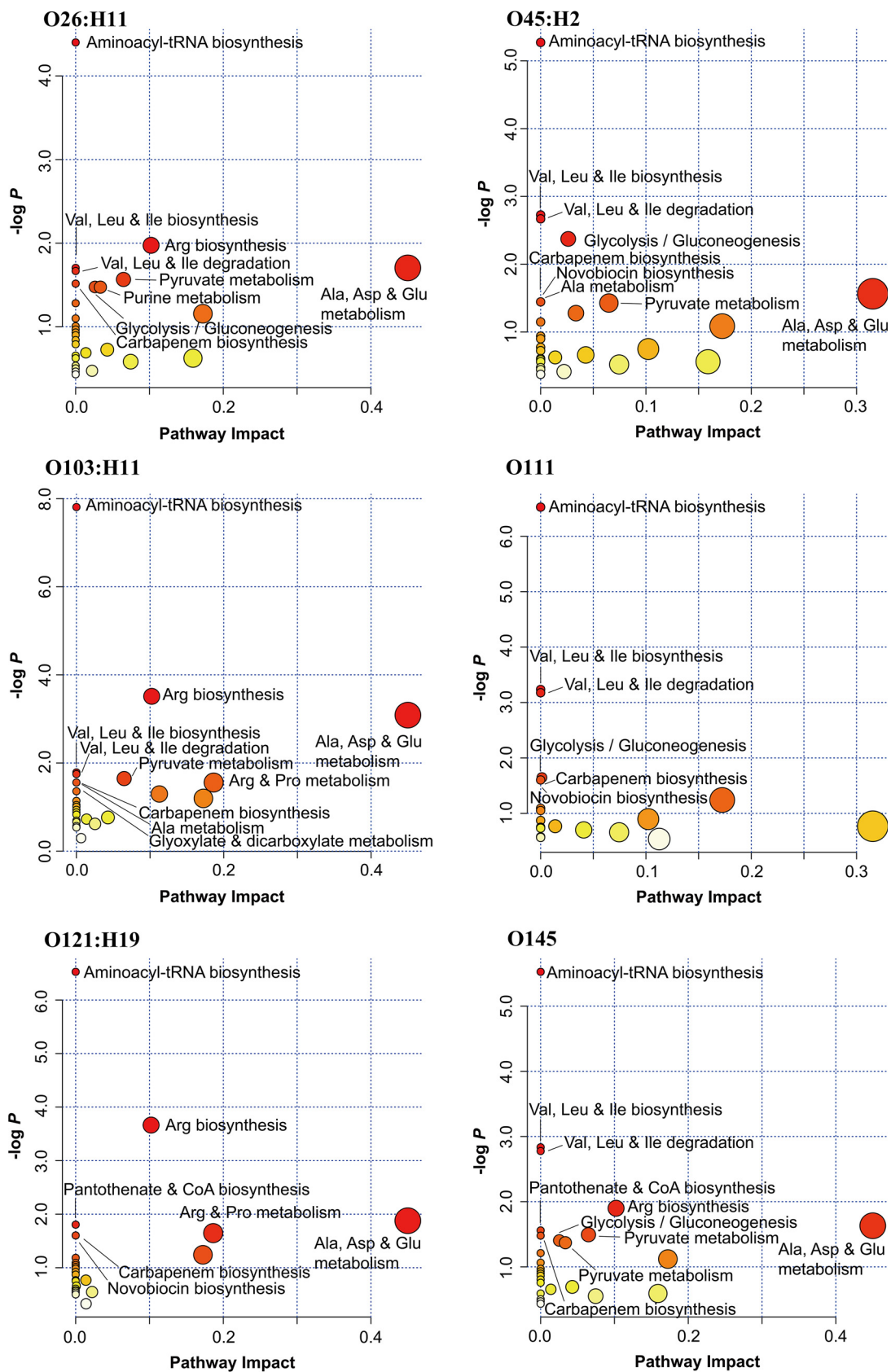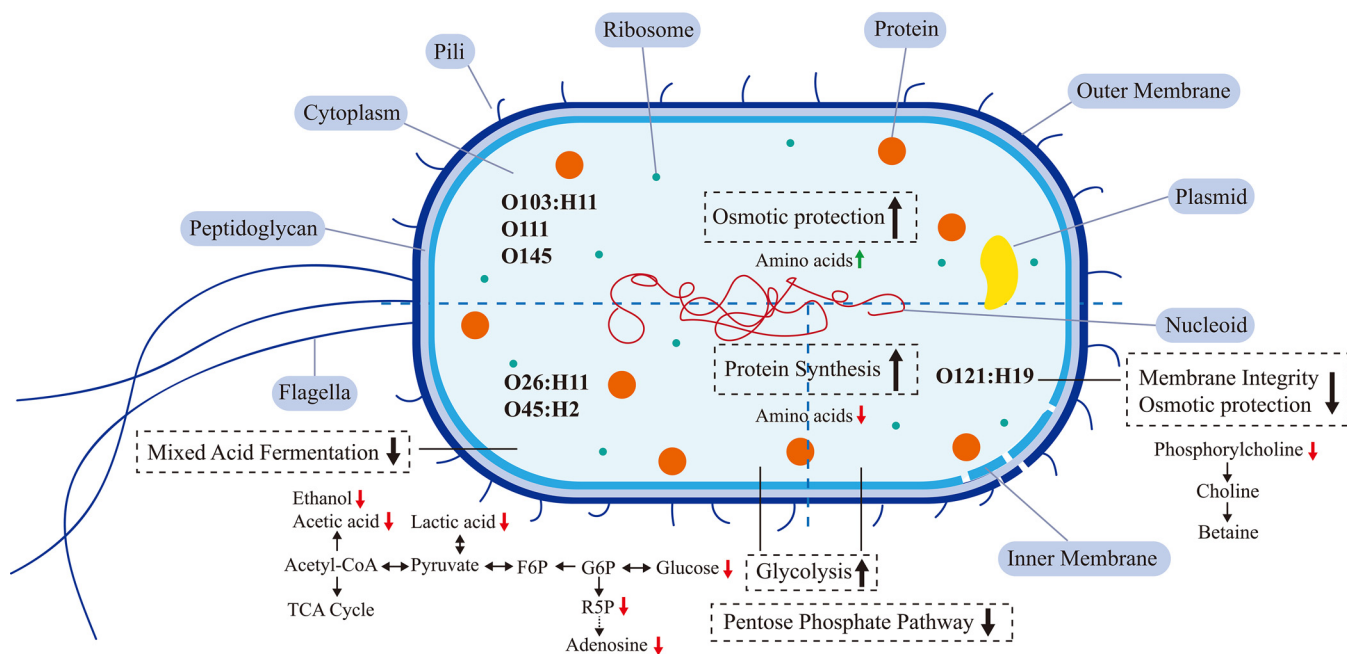
FIG 6 Metabolic pathways altered in *E. coli* O26:H11, O45:H2, O103:H11, O111, O121:H19, and O145 in wheat flour during the 60-min thermal treatment 60°C.

Serotype	Metabolic changes increasing thermal resistance	Metabolic changes decreasing thermal resistance	Resistance at 60 °C
O26:H11	Protein synthesis ↑		High
	Glycolysis ↑		
	Pentose phosphate pathway ↓		
	Mixed acid fermentation ↓		
O45:H2	Protein synthesis ↑		High
	Glycolysis ↑		
	Pentose phosphate pathway ↓		
	Mixed acid fermentation ↓		
O103:H11	Osmotic protection ↑		Moderate
O111	Osmotic protection ↑		Moderate
O145	Osmotic protection ↑		Moderate
O121:H19	Protein synthesis ↑	Membrane integrity ↓	Low
	Glycolysis ↑	Osmotic protection ↓	
	Pentose phosphate pathway ↓		

FIG 7 Schematic of metabolic alterations relevant to thermal resistance of *E. coli* O26:H11, O45:H2, O103:H11, O111, O121:H19, and O145 in wheat flour during the 60-min thermal treatment at 60°C.

phosphoglycerate kinase, hexokinase, and pyruvate kinase I, respectively, was significantly activated in *E. coli* in acidic environments, which illustrated the key role of the glycolysis pathway for energy release under stress (48). Concomitantly, significant reduction of α-D-glucose was observed in the three strains, which supported their expediting glycolysis for energy generation. Additionally, as evidenced by the noteworthy decrease of ribose-5-phosphate, the pentose phosphate pathway (PPP), which shunts from glycolysis by consuming the glycolysis intermediate glucose-6-phosphate to generate fructose-6-phosphate (49), were also influenced. Since PPP does not provide ATP, its depression would gather all available glucose into the glycolysis pathway, enabling the strains to continuously replenish the heavy energy expenditure. However,

the downregulation of PPP also brought about negative side effects. As fructose-6-phosphate is the key precursor in the biosynthesis of nucleotides (50), it was unsurprising to see that the level of adenosine significantly decreased in the three strains, which suggested a decrease in the biosynthesis of DNA and RNA as well (11). Similarly, Ye et al. also reported a significantly reduced ribose-5-phosphate level in thermally stressed *E. coli*; in that study, a massive decrease in uridine, cytidine, and adenosine was observed simultaneously (37).

Glucose consumption in O103, O111, and O145 seemed to be undisturbed throughout the heating process, as no significant glucose loss was detected. A possible reason was the abundance of amino acids remaining in the strains could provide ample substrates to energy production, which largely relieved the burden on glucose. With amino acids accumulated, osmotic protection was strengthened in the strains, which deemphasized the need for employing other defending approaches. Consequently, energy for molecular chaperone synthesis could be saved, requiring less ATP generation from glucose metabolism.

Pyruvic acid is the end product of glycolysis. In facultative anaerobes like *E. coli*, it can be metabolized downwards either to the aerobic tricarboxylic acid (TCA) cycle for energy production or to the anaerobic mixed-acid fermentation pathway for producing other organic compounds (17). The reduced level of organic acids (lactic acid and acetic acid) and/or ethanol production in O26 and O45 implied a metabolic switch from fermentation to oxidation based on the underlying principle that the TCA cycle is more energy efficient (37). In O103, O111, and O145, the TCA cycle was not reinforced, as the repression of acetic acid or ethanol production seemed to be cancelled out by the stimulated lactic acid production. This was reasonable, as ATP was not in huge demand in these strains. The alteration in the fermentation product composition was intriguing as well. Since high temperatures can cause oxygen extrusion from the media, the change in oxygen availability might have varied the fermentation preference in these strains (37, 51). Similar changes have been observed in *E. coli* BW25113 previously; in that transcriptomic study, the increased lactic acid and decreased ethanol under heat stress were attributed to the upregulation of *pflA* and *ldhA* genes and downregulation of the *adhE* gene, respectively (42). O121 was more inactive than the other strains, with both the TCA cycle and the mixed-acid fermentation remaining unmodified during the thermal treatment process. The cost of such inaction was an aggravated imbalance between the supply and demand of ATP, which hastened the demise of the O121 cells, as was observed.

In addition, a decreased phosphorylcholine level was only noticed in O121, which might be another rationale for the high vulnerability of O121 to the heat stress. Phosphorylcholine is a key membrane phospholipid precursor (52). Being involved in bilayer formation and membrane protein folding, it plays a crucial role in the maintenance of cell membrane integrity (53, 54). Moreover, phosphorylcholine can be metabolized to betaine, a molecule believed to be the most active naturally occurring osmoprotectant in *E. coli* (55). The significant decrease of phosphorylcholine in O121 strain, therefore, implied both a weakened membrane structure and an impaired osmotic protection, which in turn exposed the cells to higher magnitudes of stress.

Conclusions. The study manifests that thermal treatment is a feasible strategy for the food industry to mitigate big six *E. coli* contamination in wheat flour. Facilitated by NMR-based metabolomics, the metabolic responses of the strains underlying their different resistances at 60°C were unraveled. The O26, O45, and O121 strains shared the common metabolic changes of enhanced HSP synthesis and stimulated glycolysis, whereas the difference in osmotic protection and membrane structure intactness differentiated their thermal resistance. The O111, O145, and O103 strains also demonstrated similar metabolic alteration patterns, and their moderate thermal resistance was mainly achieved through relieving osmotic pressure by amino acid accumulation. Overall, findings from the study provide valuable insights in understanding the inactivation effect of thermal treatment against big six *E. coli* harbored in wheat flour, which

can serve as the theoretical basis for future application of thermal treatment in wheat flour production.

MATERIALS AND METHODS

***E. coli* strains and inoculum preparation.** Six *E. coli* strains, including O26:H11 (ATCC BAA-2196), O45:H2 (ATCC BAA-2193), O103:H11 (ATCC BAA-2215), O111 (ATCC BAA-2440), O121:H19 (ATCC BAA-2219), and O145 (ATCC BAA-2192), were employed in this work as representatives of the big six to enable comparison of the responses of different *E. coli* serotypes to thermal treatment. All cultures (stored in 30% glycerol at −80°C) were obtained from the Department of Food Science and Technology, National University of Singapore; before use, they were resuscitated by inoculation into 10 mL of tryptone soya broth (TSB; Oxoid, Basingstoke, UK) and incubated at 37°C overnight. The activated cultures were then acclimatized to 100 μg/mL nalidixic acid by consecutive transfers with stepwise increments in nalidixic acid concentration (56–58). Media used in the study were also supplemented with 100 μg/mL nalidixic acid to eliminate the interference of background bacteria (20).

After acclimation, the strains were individually inoculated into 100 mL of fresh TSB (1:100, vol/vol) and incubated at 37°C overnight. Cell pellets were centrifuged at 4,500 × *g* for 10 min (20°C), washed twice with 0.1% peptone water, and finally harvested in 200 μL of 0.1% peptone water. This concentrated semiliquid cell suspension was subjected to subsequent flour inoculation.

Wheat flour inoculation. The commercial all-purpose wheat flour was purchased from a local supermarket in Singapore. To minimize the influence of inoculation on the microbial thermal resistance determined in low-moisture foods (59), a concentrated cell suspension inoculation method by Forghani et al. that has been proven to barely change the a_w of wheat flour was adopted in this work (15, 16). The concentrated cell suspension of each strain prepared as described above was aseptically spot inoculated into 10 g flour in a sterile stomacher bag (Bolsa Stomacher; Deltalab, Spain) and hand mixed for 5 min. Subsequently, another 90 g flour was added to the seeded flour sample and manually mixed for 3 min, followed by two sets of stomaching (Masticator Stomacher; IUL Instruments, Germany) for 3 min and a final manual mix for 3 min. Compared to dry inoculation, which may cause variability in inoculum level, and liquid inoculation, which may affect the texture of flour (60, 61), this method could effectively deliver homogeneous microbial counts without significantly influencing the flour characteristics (15). The procedure resulted in consistent initial inoculum levels of approximately 8 log CFU/g based on the enumeration results of our pretreated samples. The pre- and postinoculation a_w of the flour samples were 0.64 ± 0.01 and 0.65 ± 0.01, respectively, as measured by a water activity meter (Aqua Lab model 3TE; Decagon Devices, Pullman, WA) at room temperature (25.2 ± 0.2°C). Since the a_w of flour was not significantly changed due to inoculation, samples were subject to subsequent thermal inactivation directly with no need to undergo an a_w reequilibration process like many other microbial thermal inactivation studies did (59, 62).

Thermal treatments. Thermal inactivation was performed at 60°C (for up to 60 min) and 70°C (for up to 20 min) using the combination of a water bath (Julabo SW22; Singapore) set two degrees higher and a block heater (Stuart Scientific, United Kingdom) set at a much higher temperature placed side by side. According to our preliminary test, this setup could significantly shorten the time for the samples to reach the target temperatures, which therefore prevented massive cell death during the temperature-rise period. Inoculated flour samples (0.60 ± 0.03 g) were weighed into 1.5-mL centrifuge tubes. They were first put in the block heater for rapid temperature increase, and upon reaching an internal temperature of 60 or 70°C, they were immediately transferred into the water bath to maintain temperature. Sample temperature was monitored using a noninoculated blank with a thermocouple located at the center (63). The come-up times, 30 and 45 s, were used as the respective zero time points (0 min) for the 60 or 70°C treatments. Starting from the 0-min samples, samples treated for 5, 10, 20, 30, 45, and 60 min at 60°C and those treated for 2.5, 5, 10, 15, and 20 min at 70°C were subsequently taken out of the water bath. Once removed, the tubes were placed in an ice-water bath immediately to quench the inactivation.

Microbiological analysis. Each tube's content was aseptically transferred to 5.4 mL 0.1% peptone water. Serial dilution was prepared and 100 μL diluent was spread plated on the nalidixic acid-supplemented tryptic soy agar (TSA; Oxoid Limited, Hampshire, UK). The colonies were enumerated after incubating at 37°C overnight and expressed as log CFU/g. To compare the antimicrobial effect against different *E. coli* strains statistically, the survival at each time point was estimated by Weibull model, $N = N_0 − (t/\delta)^{\beta}$, where N is the surviving population (log CFU/g) at time t (min), N_0 is the surviving population (log CFU/g) at 0 min, δ is the time (min) required for the first decimal reduction (min), and β is the shape parameter (15, 16, 64).

Sample size optimization for metabolomic analysis. Considering the difficulty of recovering *E. coli* cells from wheat flour, prior to the metabolomic analysis, the size of the wheat flour samples being inoculated was optimized to ensure that *E. coli* cells could be recovered in sufficient amounts for NMR analysis. O26:H11 ATCC BAA-2196 was utilized as an example strain for the optimization experiment, where each inoculum was prepared in 100 mL of TSB (1:100, vol/vol) by overnight incubation and then individually inoculated into 10, 20, 50, and 100 g of wheat flour. This amount of cells incubated, as a rule of thumb, was capable of generating recognizable NMR signals of the key metabolites in *E. coli* and other pathogens (19, 29, 32). In addition, the four sizes of wheat flour samples inoculated could all result in inoculum concentration of around 8 to 9 log CFU/g, which was the most common inoculation level utilized in wheat flour decontamination studies (65–70).

Next, to recover the *E. coli* cells, the inoculated samples were each diluted in 0.1% peptone water, thoroughly vortexed, and centrifuged at low speed (500 × *g*) for 2 min (20°C) to precipitate flour. The

supernatant then was collected while the precipitate was diluted again for another centrifugation. The process was repeated until no cell pellets were visible on the top of the precipitate. All supernatants were pooled and left to stand for 5 min to precipitate the remaining flour debris. Afterwards, the liquids were transferred to new tubes, followed by centrifugation at high speed (12,000 × *g*) for 10 min (4°C) to harvest *E. coli* cells. The recovered cells were enumerated on TSA by overnight incubation at 37°C and compared with that in the original inoculum to determine the percent recovery from different portion sizes of wheat flour. The size that resulted in the maximum recovery would be adopted for subsequent metabolomic analysis.

Metabolite extraction. Metabolomic analysis was conducted with the strains in the 60°C treated samples collected at 0, 5, and 60 min. The basic inoculation and thermal treatment procedures described in "Wheat flour inoculation" and "Thermal treatments," above, were followed, except that the size of each wheat flour sample was changed to 10 g (determined from "Sample size optimization for metabolomic analysis," above), which led to an inoculum level of approximately 9 log CFU/g, and the samples were subject to heating in 50-mL centrifuge tubes.

E. coli cells were separately recovered from samples stressed for 0, 5, and 60 min, with the same rounds of low-speed centrifugation conducted. All centrifugations were performed at 4°C. Afterwards, the cell pellets collected were immediately suspended in 1 mL of ice-cold methanol-d4 (Cambridge Isotope Laboratories, Tewksbury, MA, USA). The low temperature throughout the cell recovery process facilitated capturing the real-time metabolic profiles of the *E. coli* cells by halting the cellular enzymatic reactions and other cellular metabolic activities rapidly (71). The mixture was frozen in liquid nitrogen and then thawed on ice; the freeze-thaw cycle was repeated three times to enable complete cell membrane destruction and release of intracellular metabolites into the solvent (72–74). An overnight extraction was conducted at −20°C afterwards (75). The extract then was centrifuged at 12,000 × *g* for 20 min (4°C), and 1 mM trimethylsilyl propanoic acid (TSP; Sigma-Aldrich, Singapore) was added to the supernatant as the internal standard. After homogenizing by vortex, 600 μL of samples was transferred into 5-mm NMR tubes (Sigma-Aldrich, St. Louis, MO, USA) for immediate NMR analysis.

NMR analysis. NMR measurements were conducted on the Bruker DRX-500 NMR spectrometer (Bruker, Rheinstetten, Germany) via a triple inverse gradient probe at 298 K. The ^{1}H spectra with a width of 10.0 ppm were obtained using the standard Bruker nuclear Overhauser effect spectroscopy pulse sequence (noesypr1d), and the data were collected with an acquisition time of 3.3 s. Moreover, 128 scans and 4 dummy scans were utilized, and the relaxation delay was set at 2 s. The free induction decays were multiplied by an exponential function equivalent to a 1-Hz line-broadening factor before Fourier transformation. The 2D ^{1}H-^{13}C heteronuclear single quantum coherence (HSQC) spectrum of a representative sample was acquired using the Bruker hsqcedetgpsisp2.3 pulse sequence to facilitate metabolite identification. The ^{1}H spectra with a 10.0-ppm width and the ^{13}C spectra with a 180.0-ppm width were collected in the F2 and F1 channels, respectively (29, 55).

Spectral analysis. Baseline correction and phase distortion adjustment of all NMR spectra were manually conducted on TopSpin 4.0.9 (Bruker). The 1D ^{1}H and 2D ^{1}H-^{13}C spectra were cooperatively used for metabolite identification, and the chemical shifts were confirmed by referring to the Biological Magnetic Resonance Data Bank (http://www.bmrb.wisc.edu/metabolomics), the Human Metabolome Database (http://www.hmdb.ca/), the Madison Metabolomics Consortium Database (http://mmcd.nmrfam.wisc.edu), and relevant metabolomic studies (17, 37, 76). Afterwards, the spectra (0.5 to 10.0 ppm) excluding the methanol region (3.30 to 3.35 ppm) were normalized to the sum intensities and divided into 0.02-ppm bins using Mestrenova (Mestrelab Research SL, Santiago de Compostela, Spain) (17). Referring to the binned information, a heatmap was plotted on ClustVis (https://biit.cs.ut.ee/clustvis/) to preliminarily compare the metabolite contents of the six *E. coli* strains sampled at different time points.

While all peaks on the spectra were used for metabolite identification and quantification, those after 6.0 ppm were eliminated from further multivariate analysis due to their weak signals. This was feasible as the metabolites with peaks after 6.0 ppm also had homologous peaks in the 0.5- to 6.0-ppm region that could be processed. Principal-component analysis (PCA) and orthogonal projection to latent structures-discriminant analysis (OPLS-DA) were performed on SIMCA software (version 13.0; Umetrics, Umeå, Sweden) for group separation and pairwise comparison between different treatment times, respectively. The R^2 (representing the explained variables) and Q^2 (representing the model predictability) values were calculated to evaluate the quality of the acquired models. The OPLS-DA models were further validated by permutation test (*n* = 200) to determine if they were overfitted. The correlation coefficient and VIP values were obtained from OPLS-DA. Using the criteria of correlation coefficient of >0.602, VIP value of >1, and *P* value of <0.05 in combination, the statistically significant metabolites in differentiating the paired samples were comprehensively screened (17, 19, 77). The screened metabolites were then subject to MetaboAnalyst 5.0 (http://www.metaboanalyst.ca/) for pathway analysis to diagnose the main pathways disturbed in the thermal treatment process.

Statistical analysis. The surviving counts of the *E. coli* strains at each time point were the results of two separately inoculated 100-g flour samples, each sampled in triplicate 0.6-g portions (*n* = 6). For the optimization experiment, triplicates from separately prepared inocula were performed for each size of wheat flour sample (*n* = 3), and the averages obtained were used to plot the graph. NMR analysis at each sampling time point was also performed in triplicates independently using separately prepared inocula (*n* = 3). One-way analysis of variance (ANOVA) and least significant difference (LSD) were conducted in SAS 9.4 (Statistical Analysis System, Cary, NC) to compare the effects of thermal treatment against the different *E. coli* strains in wheat flour. The significance of difference was defined at a *P* value of <0.05.

SUPPLEMENTAL MATERIAL

Supplemental material is available online only.

SUPPLEMENTAL FILE 1, PDF file, 1.1 MB.

ACKNOWLEDGMENTS

REFERENCES

1. US Department of Agriculture. 2019. Wheat, durum. https://fdc.nal.usda.gov/index.html.

2. Shewry PR, Halford NG, Belton PS, Tatham AS. 2002. The structure and properties of gluten: an elastic protein from wheat grain. Philos Trans R Soc Lond B Biol Sci 357:133–142. https://doi.org/10.1098/rstb.2001.1024.

3. Shewry PR, Hey SJ. 2015. The contribution of wheat to human diet and health. Food Energy Secur 4:178–202. https://doi.org/10.1002/fes3.64.

4. Food and Agriculture Organization of the United Nations. 2021. FAOSTAT. http://www.fao.org/faostat/en/#data/QC.

5. Food and Agriculture Organization of the United Nations. 2021. World food situation: FAO cereal supply and demand brief. http://www.fao.org/worldfoodsituation/csdb/en/.

6. Manthey FA, Wolf-Hall CE, Yalla S, Vijayakumar C, Carlson D. 2004. Microbial loads, mycotoxins, and quality of durum wheat from the 2001 harvest of the northern plains region of the United States. J Food Prot 67:772–780. https://doi.org/10.4315/0362-028x-67.4.772.

7. Centers for Disease Control and Prevention. 2016. O121 and O26 infections linked to flour. https://www.cdc.gov/ecoli/2016/o121-06-16/index.html.

8. Centers for Disease Control and Prevention. 2019. Outbreak of *E. coli* infections linked to flour. https://www.cdc.gov/ecoli/2019/flour-05-19/index.html.

9. Centers for Disease Control and Prevention. 2021. *E. coli* outbreak linked to cake mix. https://www-cdc-gov.libproxy1.nus.edu.sg/ecoli/2021/o121-07-21/index.html.

10. Forghani F, Li S, Zhang S, Mann DA, Deng X, den Bakker HC, Diez-Gonzalez F. 2020. *Salmonella enterica* and *Escherichia coli* in wheat flour: detection and serotyping by a quasimetagenomic approach assisted by magnetic capture, multiple-displacement amplification, and real-time sequencing. Appl Environ Microbiol 86:e00097-20. https://doi.org/10.1128/AEM.00097-20.

11. Liu Q, Chen L, Laserna AKC, He Y, Feng X, Yang H. 2020. Synergistic action of electrolyzed water and mild heat for enhanced microbial inactivation of *Escherichia coli* O157:H7 revealed by metabolomics analysis. Food Control 110:107026. https://doi.org/10.1016/j.foodcont.2019.107026.

12. Wu J, Zhao L, Lai S, Yang H. 2021. NMR-based metabolomic investigation of antimicrobial mechanism of electrolysed water combined with moderate heat treatment against *Listeria monocytogenes* on salmon. Food Control 125:107974. https://doi.org/10.1016/j.foodcont.2021.107974.

13. Daryaei H, Peñaloza W, Hildebrandt I, Krishnamurthy K, Thiruvengadam P, Wan J. 2018. Heat inactivation of Shiga toxin-producing *Escherichia coli* in a selection of low moisture foods. Food Control 85:48–56. https://doi.org/10.1016/j.foodcont.2017.08.029.

14. Daryaei H, Sui Q, Liu H, Rehkopf A, Peñaloza W, Rytz A, Luo Y, Wan J. 2020. Heat resistance of Shiga toxin-producing *Escherichia coli* and potential surrogates in wheat flour at two moisture levels. Food Control 108:106788. https://doi.org/10.1016/j.foodcont.2019.106788.

15. Forghani F, Bakker M, Futral AN, Diez-Gonzalez F. 2018. Long-term survival and thermal death kinetics of enterohemorrhagic *Escherichia coli* serogroups O26, O103, O111, and O157 in wheat flour. Appl Environ Microbiol 84:e00283-18. https://doi.org/10.1128/AEM.00283-18.

16. Forghani F, den Bakker M, Liao JY, Payton AS, Futral AN, Diez-Gonzalez F. 2019. Salmonella and enterohemorrhagic *Escherichia coli* serogroups O45, O121, O145 in wheat flour: effects of long-term storage and thermal treatments. Front Microbiol 10:323. https://doi.org/10.3389/fmicb.2019.00323.

17. Chen L, Zhao X, Wu J, Liu Q, Pang X, Yang H. 2020. Metabolic characterisation of eight *Escherichia coli* strains including "big six" and acidic responses of selected strains revealed by NMR spectroscopy. Food Microbiol 88:103399. https://doi.org/10.1016/j.fm.2019.103399.

18. Zhao X, Chen L, Wu J, He Y, Yang H. 2020. Elucidating antimicrobial mechanism of nisin and grape seed extract against *Listeria monocytogenes* in broth and on shrimp through NMR-based metabolomics approach. Int J Food Microbiol 319:108494. https://doi.org/10.1016/j.ijfoodmicro.2019.108494.

19. Liu Q, Wu J, Lim ZY, Lai S, Lee N, Yang H. 2018. Metabolite profiling of Listeria innocua for unravelling the inactivation mechanism of electrolysed water by nuclear magnetic resonance spectroscopy. Int J Food Microbiol 271:24–32. https://doi.org/10.1016/j.ijfoodmicro.2018.02.014.

20. Liu Q, Tan CSC, Yang H, Wang S. 2017. Treatment with low-concentration acidic electrolysed water combined with mild heat to sanitise fresh organic broccoli (Brassica oleracea). LWT Food Sci Technol 79:594–600. https://doi.org/10.1016/j.lwt.2016.11.012.

21. Suehr QJ, Anderson NM, Keller SE. 2019. Desiccation and thermal resistance of *Escherichia coli* O121 in wheat flour. J Food Prot 82:1308–1313. https://doi.org/10.4315/0362-028X.JFP-18-544.

22. Van Steertegem B, Pareyt B, Slade L, Levine H, Brijs K, Delcour JA. 2013. Impact of heat treatment on wheat flour solvent retention capacity (SRC) profiles. Cereal Chem 90:608–610. https://doi.org/10.1094/CCHEM-04-13-0069-N.

23. Keppler S, Bakalis S, Leadley CE, Sahi SS, Fryer PJ. 2018. Evaluation of dry heat treatment of soft wheat flour for the production of high ratio cakes. Food Res Int 107:360–370. https://doi.org/10.1016/j.foodres.2018.02.041.

24. Liu Q, Jin X, Feng X, Yang H, Fu C. 2019. Inactivation kinetics of *Escherichia coli* O157:H7 and *Salmonella* Typhimurium on organic carrot (Daucus carota L.) treated with low concentration electrolyzed water combined with short-time heat treatment. Food Control 106:106702. https://doi.org/10.1016/j.foodcont.2019.06.028.

25. Adhikari A, Syamaladevi RM, Killinger K, Sablani SS. 2015. Ultraviolet-C light inactivation of *Escherichia coli* O157: H7 and *Listeria monocytogenes* on organic fruit surfaces. Int J Food Microbiol 210:136–142. https://doi.org/10.1016/j.ijfoodmicro.2015.06.018.

26. Mackey BM, Derrick C. 1990. Heat shock protein synthesis and thermotolerance in *Salmonella typhimurium*. J Appl Bacteriol 69:373–383. https://doi.org/10.1111/j.1365-2672.1990.tb01527.x.

27. Mackey BM, Derrick CM. 1987. Changes in the heat resistance of *Salmonella typhimurium* during heating at rising temperatures. Lett Appl Microbiol 4:13–16. https://doi.org/10.1111/j.1472-765X.1987.tb01571.x.

28. Peterson CN, Mandel MJ, Silhavy TJ. 2005. Escherichia coli starvation diets: essential nutrients weigh in distinctly. J Bacteriol 187:7549–7553. https://doi.org/10.1128/JB.187.22.7549-7553.2005.

29. He Y, Zhao X, Chen L, Zhao L, Yang H. 2021. Effect of electrolysed water generated by sodium chloride combined with sodium bicarbonate solution against *Listeria innocua* in broth and on shrimp. Food Control 127:108134. https://doi.org/10.1016/j.foodcont.2021.108134.

30. Fontana JA. 2007. Appendix D: minimum water activity limits for growth of microorganisms, p 405. *In* Water activity in foods. Blackwell Publishing, Hoboken, NJ. https://doi.org/10.1002/9780470376454.app4.

31. Al-Holy MA, Rasco BA. 2015. The bactericidal activity of acidic electrolyzed oxidizing water against *Escherichia coli* O157:H7, *Salmonella* Typhimurium, and *Listeria monocytogenes* on raw fish, chicken and beef surfaces. Food Control 54:317–321. https://doi.org/10.1016/j.foodcont.2015.02.017.

32. Wang Y, Wu J, Yang H. 2022. Comparison of the metabolic responses of eight *Escherichia coli* strains including the "big six" in pea sprouts to low concentration electrolysed water by NMR spectroscopy. Food Control 131:108458. https://doi.org/10.1016/j.foodcont.2021.108458.

33. Sapers GM, Miller RL, Mattrazzo AM. 1999. Effectiveness of sanitizing agents in inactivating *Escherichia coli* in golden delicious apples. J Food Sci 64:734–737. https://doi.org/10.1111/j.1365-2621.1999.tb15121.x.

34. Venkitanarayanan KS, Lin C-M, Bailey H, Doyle MP. 2002. Inactivation of *Escherichia coli* O157:H7, *Salmonella* Enteritidis, and *Listeria monocytogenes* on apples, oranges, and tomatoes by lactic acid with hydrogen peroxide. J Food Prot 65:100–105. https://doi.org/10.4315/0362-028x-65.1.100.

35. Park SH, Choi MR, Park JW, Park KH, Chung MS, Ryu S, Kang DH. 2011. Use of organic acids to inactivate *Escherichia coli* O157:H7, *Salmonella* Typhimurium, and *Listeria monocytogenes* on organic fresh apples and lettuce. J Food Sci 76: M293–M298. https://doi.org/10.1111/j.1750-3841.2011.02205.x.

36. Zook CD, Busta FF, Brady LJ. 2001. Sublethal sanitizer stress and adaptive response of *Escherichia coli* O157:H7. J Food Prot 64:767–769. https://doi.org/10.4315/0362-028x-64.6.767.

37. Ye Y, Zhang L, Hao F, Zhang J, Wang Y, Tang H. 2012. Global metabolomic responses of *Escherichia coli* to heat stress. J Proteome Res 11:2559–2566. https://doi.org/10.1021/pr3000128.

38. Yuk HG, Marshall DL. 2003. Heat adaptation alters *Escherichia coli* O157:H7 membrane lipid composition and verotoxin production. Appl Environ Microbiol 69:5115–5119. https://doi.org/10.1128/AEM.69.9.5115-5119.2003.

39. Wang S, Deng K, Zaremba S, Deng X, Lin C, Wang Q, Tortorello ML, Zhang W. 2009. Transcriptomic response of *Escherichia coli* O157:H7 to oxidative stress. Appl Environ Microbiol 75:6110–6123. https://doi.org/10.1128/AEM.00914-09.

40. Ponomarenko M, Stepanenko I, Kolchanov N. 2013. Heat shock proteins, p 402–405. *In* Maloy S, Hughes K (ed), Brenner's encyclopedia of genetics, 2nd ed. Academic Press, San Diego, CA. https://doi.org/10.1016/B978-0-12-374984-0.00685-9.

41. Nonaka G, Blankschien M, Herman C, Gross CA, Rhodius VA. 2006. Regulon and promoter analysis of the *E. coli* heat-shock factor, sigma32, reveals a multifaceted cellular response to heat stress. Genes Dev 20: 1776–1789. https://doi.org/10.1101/gad.1428206.

42. Hasan CMM, Shimizu K. 2008. Effect of temperature up-shift on fermentation and metabolic characteristics in view of gene expressions in *Escherichia coli*. Microb Cell Fact 7:35. https://doi.org/10.1186/1475-2859-7-35.

43. Li SS, Hu X, Zhao H, Li YX, Zhang L, Gong LJ, Guo J, Zhao HB. 2015. Quantitative analysis of cellular proteome alterations of *Pseudomonas putida* to naphthalene-induced stress. Biotechnol Lett 37:1645–1654. https://doi.org/10.1007/s10529-015-1828-y.

44. Tian X, Yu Q, Wu W, Li X, Dai R. 2018. Comparative proteomic analysis of *Escherichia coli* O157:H7 following ohmic and water bath heating by capillary-HPLC-MS/MS. Int J Food Microbiol 285:42–49. https://doi.org/10.1016/j.ijfoodmicro.2018.06.005.

45. Lu H, Ulanov AV, Nobu M, Liu WT. 2016. Global metabolomic responses of *Nitrosomonas europaea* 19718 to cold stress and altered ammonia feeding patterns. Appl Microbiol Biotechnol 100:1843–1852. https://doi.org/10.1007/s00253-015-7095-y.

46. Jozefczuk S, Klie S, Catchpole G, Szymanski J, Cuadros-Inostroza A, Steinhauser D, Selbig J, Willmitzer L. 2010. Metabolomic and transcriptomic stress response of *Escherichia coli*. Mol Syst Biol 6:364. https://doi.org/10.1038/msb.2010.18.

47. Khan SH, Ahmad N, Ahmad F, Kumar R. 2010. Naturally occurring organic osmolytes: from cell physiology to disease prevention. IUBMB Life 62: 891–895. https://doi.org/10.1002/iub.406.

48. Zhang W, Chen X, Sun W, Nie T, Quanquin N, Sun Y. 2020. *Escherichia coli* increases its ATP concentration in weakly acidic environments principally through the glycolytic pathway. Genes 11:991. https://doi.org/10.3390/genes11090991.

49. Ge T, Yang J, Zhou S, Wang Y, Li Y, Tong X. 2020. The role of the pentose phosphate pathway in diabetes and cancer. Front Endocrinol (Lausanne) 11:365. https://doi.org/10.3389/fendo.2020.00365.

50. Stincone A, Prigione A, Cramer T, Wamelink MMC, Campbell K, Cheung E, Olin-Sandoval V, Grüning N-M, Krüger A, Tauqeer Alam M, Keller MA, Breitenbach M, Brindle KM, Rabinowitz JD, Ralser M. 2015. The return of metabolism: biochemistry and physiology of the pentose phosphate pathway. Biol Rev Camb Philos Soc 90:927–963. https://doi.org/10.1111/brv.12140.

51. Soini J, Falschlehner C, Mayer C, Böhm D, Weinel S, Panula J, Vasala A, Neubauer P. 2005. Transient increase of ATP as a response to temperature up-shift in *Escherichia coli*. Microb Cell Fact 4:9. https://doi.org/10.1186/1475-2859-4-9.

52. Geiger O, López-Lara IM, Sohlenkamp C. 2013. Phosphatidylcholine biosynthesis and function in bacteria. Biochim Biophys Acta 1831:503–513. https://doi.org/10.1016/j.bbalip.2012.08.009.

53. Bogdanov M, Umeda M, Dowhan W. 1999. Phospholipid-assisted refolding of an integral membrane protein: minimum structural features for phosohatidylethanolamine to act as a molecular chaperone. J Biol Chem 274:12339–12345. https://doi.org/10.1074/jbc.274.18.12339.

54. Sohlenkamp C, López-Lara IM, Geiger O. 2003. Biosynthesis of phosphatidylcholine in bacteria. Prog Lipid Res 42:115–162. https://doi.org/10.1016/s0163-7827(02)00050-4.

55. Zhao L, Zhao X, Wu J, Lou X, Yang H. 2019. Comparison of metabolic response between the planktonic and air-dried *Escherichia coli* to electrolysed water combined with ultrasound by ^{1}H NMR spectroscopy. Food Res Int 125:108607. https://doi.org/10.1016/j.foodres.2019.108607.

56. Mendonca AF, Reitmeier CA, Sikinyi T. 2004. Evaluation of a GRAS sanitizer for enhanced microbial safety and shelf-life of whole tomatoes for ISS and planetary outpost. SAE Trans 113:1321–1329.

57. Parnell TL, Harris LJ, Suslow TV. 2005. Reducing *Salmonella* on cantaloupes and honeydew melons using wash practices applicable to postharvest handling, foodservice, and consumer preparation. Int J Food Microbiol 99:59–70. https://doi.org/10.1016/j.ijfoodmicro.2004.07.014.

58. Kharel K, Adhikari A, Graham CJ, Prinyawiwatkul W, Yemmireddy VK. 2018. Hot water treatment as a kill-step to inactivate *Escherichia coli* O157:H7, *Salmonella enterica*, *Listeria monocytogenes* and *Enterococcus faecium* on in-shell pecans. LWT Food Sci Technol 97:555–560. https://doi.org/10.1016/j.lwt.2018.07.048.

59. Hildebrandt IM, Marks BP, Ryser ET, Villa-Rojas R, Tang J, Garces-Vega FJ, Buchholz SE. 2016. Effects of inoculation procedures on variability and repeatability of *Salmonella* thermal resistance in wheat flour. J Food Prot 79:1833–1839. https://doi.org/10.4315/0362-028X.JFP-16-057.

60. Beuchat LR, Mann DA, Kelly CA, Ortega YR. 2017. Retention of viability of *Salmonella* in sucrose as affected by type of inoculum, water activity, and storage temperature. J Food Prot 80:1408–1414. https://doi.org/10.4315/0362-028X.JFP-16-537.

61. Blessington T, Theofel CG, Harris LJ. 2013. A dry-inoculation method for nut kernels. Food Microbiol 33:292–297. https://doi.org/10.1016/j.fm.2012.09.009.

62. Hildebrandt IM, Marks BP, Anderson NM, Grasso-Kelley EM. 2020. Reproducibility of *Salmonella* thermal resistance measurements via multilaboratory isothermal inactivation experiments. J Food Prot 83:609–614. https://doi.org/10.4315/0362-028X.JFP-19-343.

63. Smith DF, Hildebrandt IM, Casulli KE, Dolan KD, Marks BP. 2016. Modeling the effect of temperature and water activity on the thermal resistance of *Salmonella enteritidis* PT 30 in wheat flour. J Food Prot 79:2058–2065. https://doi.org/10.4315/0362-028X.JFP-16-155.

64. Chen L, Zhang H, Liu Q, Pang X, Zhao X, Yang H. 2019. Sanitising efficacy of lactic acid combined with low-concentration sodium hypochlorite on *Listeria innocua* in organic broccoli sprouts. Int J Food Microbiol 295: 41–48. https://doi.org/10.1016/j.ijfoodmicro.2019.02.014.

65. Du L, Jaya Prasad A, Gänzle M, Roopesh MS. 2020. Inactivation of *Salmonella* spp. in wheat flour by 395 nm pulsed light emitting diode (LED) treatment and the related functional and structural changes of gluten. Food Res Int 127:108716. https://doi.org/10.1016/j.foodres.2019.108716.

66. Fine F, Gervais P. 2004. Efficiency of pulsed UV light for microbial decontamination of food powders. J Food Prot 67:787–792. https://doi.org/10.4315/0362-028x-67.4.787.

67. Liu S, Ozturk S, Xu J, Kong F, Gray P, Zhu M-J, Sablani SS, Tang J. 2018. Microbial validation of radio frequency pasteurization of wheat flour by inoculated pack studies. J Food Eng 217:68–74. https://doi.org/10.1016/j.jfoodeng.2017.08.013.

68. Subedi S, Du L, Prasad A, Yadav B, Roopesh MS. 2020. Inactivation of *Salmonella* and quality changes in wheat flour after pulsed light-emitting diode (LED) treatments. Food Bioprod Process 121:166–177. https://doi.org/10.1016/j.fbp.2020.02.004.

69. Villa-Rojas R, Zhu M-J, Marks BP, Tang J. 2017. Radiofrequency inactivation of *Salmonella* Enteritidis PT 30 and *Enterococcus faecium* in wheat flour at different water activities. Biosys Eng 156:7–16. https://doi.org/10.1016/j.biosystemseng.2017.01.001.

70. Xu J, Liu S, Tang J, Ozturk S, Kong F, Shah DH. 2018. Application of freeze-dried *Enterococcus faecium* NRRL B-2354 in radio-frequency pasteurization of wheat flour. LWT 90:124–131. https://doi.org/10.1016/j.lwt.2017.12.014.

71. Sellick CA, Hansen R, Stephens GM, Goodacre R, Dickson AJ. 2011. Metabolite extraction from suspension-cultured mammalian cells for global

metabolite profiling. Nat Protoc 6:1241–1249. https://doi.org/10.1038/nprot.2011.366.

72. Winder CL, Dunn WB, Schuler S, Broadhurst D, Jarvis R, Stephens GM, Goodacre R. 2008. Global metabolic profiling of *Escherichia coli* cultures: an evaluation of methods for quenching and extraction of intracellular metabolites. Anal Chem 80:2939–2948. https://doi.org/10.1021/ac7023409.

73. Jäpelt KB, Nielsen NJ, Wiese S, Christensen JH. 2015. Metabolic fingerprinting of *Lactobacillus paracasei*: a multi-criteria evaluation of methods for extraction of intracellular metabolites. Anal Bioanal Chem 407:6095–6104. https://doi.org/10.1007/s00216-015-8783-2.

74. Schatschneider S, Abdelrazig S, Safo L, Henstra AM, Millat T, Kim DH, Winzer K, Minton NP, Barrett DA. 2018. Quantitative isotope-dilution high-resolution-mass-spectrometry analysis of multiple intracellular metabolites in *Clostridium autoethanogenum* with uniformly ^{13}C-labeled standards derived from spirulina. Anal Chem 90:4470–4477. https://doi.org/10.1021/acs.analchem.7b04758.

75. Pinu FR, Villas-Boas SG, Aggio R. 2017. Analysis of intracellular metabolites from microorganisms: quenching and extraction protocols. Metabolites 7:53. https://doi.org/10.3390/metabo7040053.

76. Liu Q, Wu J, Lim ZY, Aggarwal A, Yang H, Wang S. 2017. Evaluation of the metabolic response of *Escherichia coli* to electrolysed water by ^{1}H NMR spectroscopy. LWT Food Sci Technol 79:428–436. https://doi.org/10.1016/j.lwt.2017.01.066.

77. Lou X, Zhai D, Yang H. 2021. Changes of metabolite profiles of fish models inoculated with *Shewanella baltica* during spoilage. Food Control 123:107697. https://doi.org/10.1016/j.foodcont.2020.107697.